DEGREE PROJECT, IN MECHATRONICS , FIRST LEVEL
STOCKHOLM, *SWEDEN 2015*

Automatic robot gripping claw

AUTOMATISERAD ROBOT GRIPKLO

MATTHIAS CARLSSON

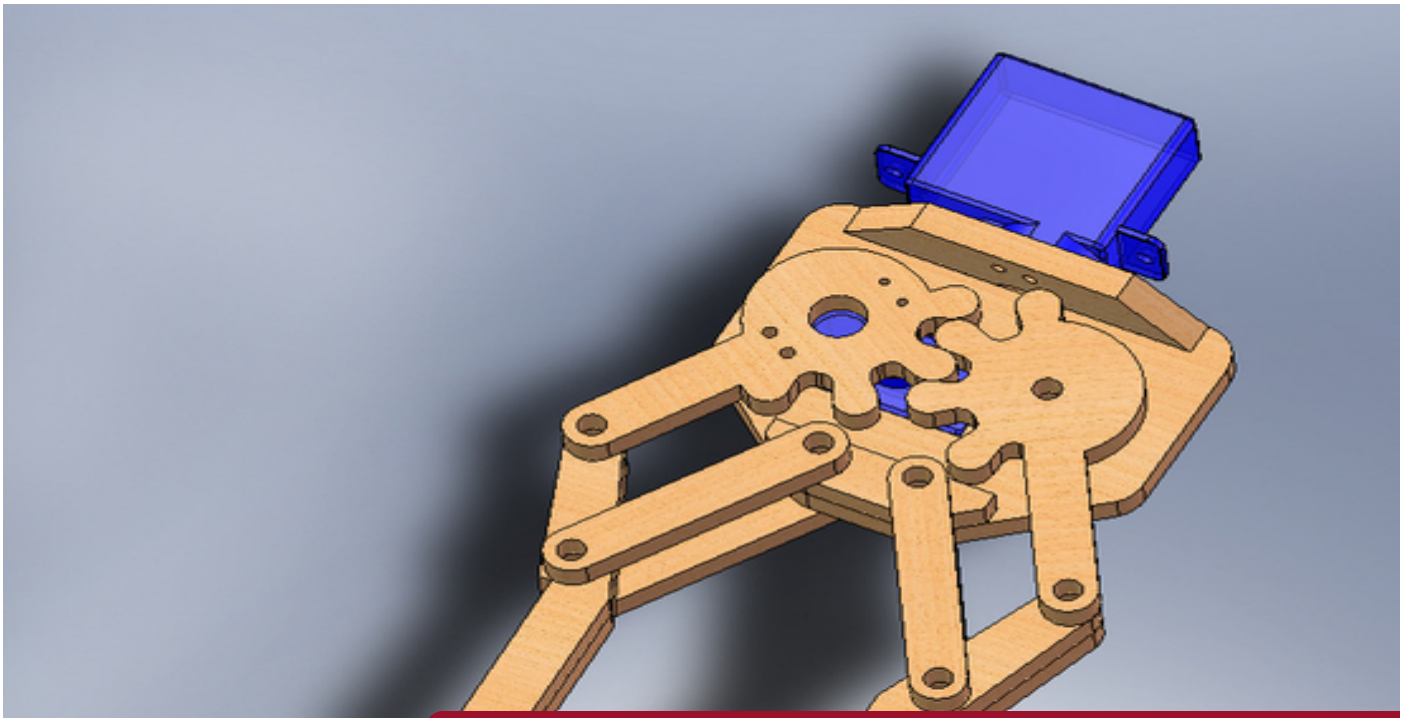

KTH ROYAL INSTITUTE OF TECHNOLOGY

SCHOOL OF INDUSTRIAL ENGINEERING AND MANAGEMENT

Automatic robotic gripping claw

MATTHIAS CARLSSON

Bacherlor's Thesis in Mechatronics

Supervisor:	Baha Alhaj Hasan
Examiner:	Martin Edin Grimheden
Approved:	2015-month-day

TRITA MMK 2015-23

Abstract

In industrial production, automatization is a common concept utilized in a range of applications where time dependency is a key factor. The robotic arm is one of the tools applied in the area and its extension, such as a robotic claw, affects the execution and the accuracy of the robotics.
This paper researches whether infrared- or ultrasonic sensors are best suited for the automation of a robotic claw, created out of 3D-printing and wooden material; in terms of time delay and object-size prediction. With help of a simple physical model and a sphere in motion the resulting time delay could be determined to be larger in ultrasonic sensors, while both were unable to provide accurate object measurement predictions. The research proved the infrared sensor better abilities in motion based automation.

Sammanfattning

Automatiserad robot gripklo

Inom industriall produktion är automatisering ett vanligt utnyttjat koncept i ett urval applikationer där tidsberoendet är en nyckelfaktor. Robotarmen är ett av verktygen som uttnyttjas inom området och dess förlängning, såsom en robotklo, påverkar utförandet och noggrannheten hos robotiken.
Den här uppsatsen undersöker huruvida infraröda- eller ultraljuds sensorer är bäst lämpade för automatisering av en robotklo, skapad via en 3D-printer och trämaterial; gällande tidsfördröjning och förutseendet av objektets storlek. Med hjälp av en simpel fysisk modell och en sfär i rörelse; kunde den resulterande tidsfödröjningen bekräftas större med ultrasonisk sensor, medan ingen utav sensorerna kunde ytföra noggranna beräkningar av objektet. Undersökningen kunde bevisa att infraröda sensorer innehar bättre egenskaper inom rörelsebaserad automation.

Preface

I would like to thank David Broman for inspiration regarding the research subject and Baha Alhaj Hasan for counseling throughout the project.

Matthias Carlsson
Stockholm, May, 2015

Contents

Nomenclature

Symbols

Symbols	Description
t	Time (s)
τ	Time delay
F	Total force (N)
m	Mass (kg)
x	Displacement x-axis (m)
y	Displacement y-axis (m)
v	Velocity (m/s)
a	Accleration (m/s^2)
c_{air}	Air velocity (m/s)
c_{light}	Light velocity (m/s)
H	Handwheel in electrical motor
L	Load in electrical motor
θ	Angle (°)
I	Current (A)
V	Voltage (V)
r	Radius (m)

Abbreviations

Abbreviation	Description
IR	Infrared light
CAD	Computer Aided Design
PWM	Pulse Width Modulation
I/O	Input/Output
Vcc	IC power-supply pin
GND	Ground
EPS	Expanded Polystyrene
KTH	Kungliga Tekniska Högskolan
LED	Light-emitting diode
CPU	Central processing unit

Chapter 1

Introduction

In this chapter an introduction to the thesis is given and the purpose, scope and methods used explained.

1.1 Background

In industry there is an increasing demand of automatized tools to enhance the efficiency of production. A key element is the robotic arm [Karlsson, 2013] [Alpman, 2014], which has a broad range of applications dependent on its extension that can be applied in a variety of scenarios. The extension's accuracy and functionality are of vital importance for the system and the final execution of the automation. This thesis evaluates a constructed robotic claw and examines the functionality and abilities while it is automatically controlled by sensors to perform a timed grip.

1.2 Purpose

This project utilizes an automatized mechanical gripping claw, controlled by a motor and activated by distance sensors, to catch a moving object of unknown size and researching the reaction time dependence between different types of sensors and the success in gripping the object. The conclusion focuses on available improvements in both software and hardware.
Additionally the robotic claw aims to function as an extension to a robot arm, created via a master's thesis by Viktor Kozma, supervised and requested by David Broman [Broman, 2015].

1.3 Scope

The budget of the project limits the amount of sensors to three of each. As a result the moving objects evaluated are limited to spheres, with constant acceleration and with one dimensional motion. The robotic claw's size is designed in correlation to the robot arm and the maximum theoretical radius of any object is limited to 5 cm.

Effects from friction, wind and material properties are assumed to be homogeneous and neglected. Temperature is constantly assumed to be 20 °C.

1.4 Method

Two different balls made out of glass with radius of 1.25 cm and 1.75 cm, is put in motion on a ramp with a small gap enabling the ball to sustain a one dimensional motion. The motion is set to fixed velocities dependent on the angle of ramp of 4 °and 10.5 °. Three sensors are placed with a specific distance between each other, with varying orthogonal length from the object's trajectory. A simple picture explaining the method can be seen in Fig. 1.1 and 1.2
The success in gripping the moving object is evaluated for each initial velocity and distance from the track. The measured radius by the system and the actual radius is compared. The time for the grip to be performed and the time the object appears at a sensor placed behind the robotic claw that measures the exact time when the object was present is compared. The combined results are evaluated for the overall success of the grip.

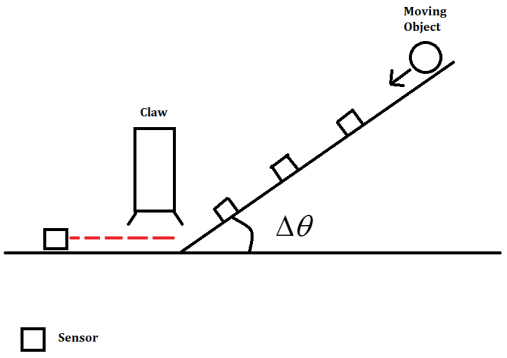

Figure 1.1: Simple picture for the experimental set up, side view.

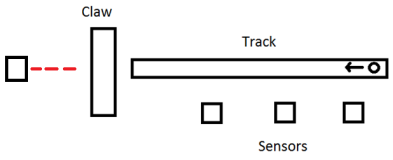

Figure 1.2: Simple picture for the experimental set up, top view.

Chapter 2

Theory

This chapter presents the theory needed for the project.

2.1 Motion of the object

Through the derivatives of displacements a model can be applied to calculate the displacement x_i dependent on time t

$$x_i(t) = x_{i-1} + v_{i-1}\Delta t + \frac{1}{2}a_{i-1}\Delta t^2, i = (1, 2...n) \tag{2.1}$$

where v_i is the velocity and a_i is the acceleration. By assuming no additional forces are applied during the motion, the resulting acceleration becomes constant according to Newton's second law

$$\frac{\Delta \mathbf{F}(t)}{m} = \Delta a = 0 \Rightarrow a_i = constant = \frac{v_i - v_{i-1}}{\Delta t} \tag{2.2}$$

which in turn reduces the equation for velocity to

$$\Delta a = 0 \Rightarrow v_i = \frac{x_i - x_{i-1}}{\Delta t} \tag{2.3}$$

according to [Murdock, 2000] .
With known displacements $\mathbf{x} = (x_1, ..., x_n)$ and boundary values from equation 2.2-2.3, the model from equation 2.1 can be solved for time as a second degree polynomial

$$\Delta t = \frac{-v_{i-1}}{2\frac{a_{i-1}}{2}} \pm \sqrt{(\frac{-v_{i-1}}{2\frac{a_{i-1}}{2}})^2 - \frac{(x_{i-1} - x_i)}{\frac{a_{i-1}}{2}}} \tag{2.4}$$

2.2 Ultrasonic distance Sensor

Several distance sensors function through using a transmitter and a receiver, such as the ultrasonic sensor. The transmitter sends a signal forward that reflects back to the receiver. If the sensor detects an object in the pulse's path it digitally transmits the information through varying the voltage output of the signal sent from the sensor.
The ultrasonic sensor transmits pulses of ultrasound which means that the signals travel in the speed of sound c_{air} with the value $340m/s$. With trivial physics the distance between the sensor and the object can be calculated as

$$r_T = \frac{c_{air}\tau_{ping}}{2} \tag{2.5}$$

where r_T is the radius of the pulse and τ_{ping} is the time for the receiver to read a signal after the transmitter sends a pulse. The distance is then reduced by half due to the reflection projecting a doubled distance from reality. [elecfreaks, 2011]
A visualization of the ultrasonic sensor's function can be seen in Fig. 2.1 .

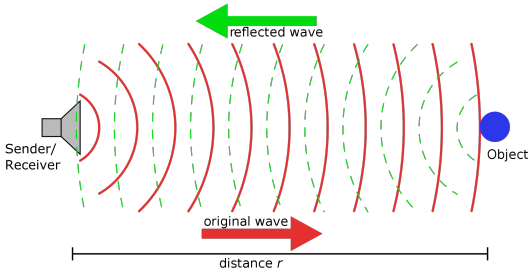

Figure 2.1: Ultrasonic sensor detection [Wong, 2011].

2.3 Infrared distance sensor

The infrared sensor is another type of sensor that can be utilized in range detection. The transmitter outputs a concentrated flash of light from an LED at a certain IR wavelength which reflects back whenever it reaches an object. The receiver measures the intensity of the reflected light and outputs a voltage proportional to it [RoboticsAcademy, 1999].
A picture with the working principles of IR-light can be seen in Fig. 2.2

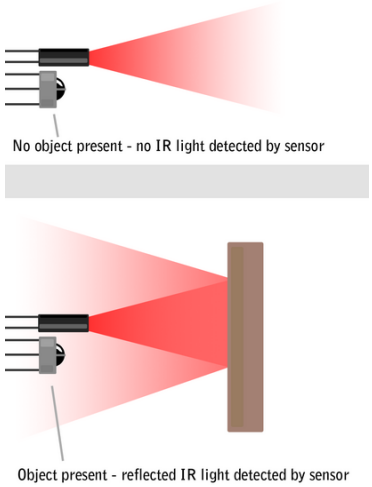

Figure 2.2: Infrared sensor detection [RoboticsAcademy, 1999].

2.4 Servo motor

For controlled electrical motor operations, servo motors can be utilized. The servo motor is a type of DC motor with a potentiometer, additional gear arrangement and feedback circuitry. The result becomes an electrical motor that can generate a high torque, with high precision rotation at a low speed. The servo motor functions are opposite of those of the typical DC motor which generates a high speed rotation with low torque in an open system [Getting, 2015]. Fig. 2.3 and 2.4 shows a simple schematics comparison between a closed- and an open system for an electrical motor. Servo motors activates with Pulse Width Modulation. The length of the pulse determines the angle of rotation for the servo's rotor. Additionally the frequency of the pulse contributes to a time delay which has to be accounted for. The frequencies and specific pulse widths are specified in data sheets or could be experimentally determined.

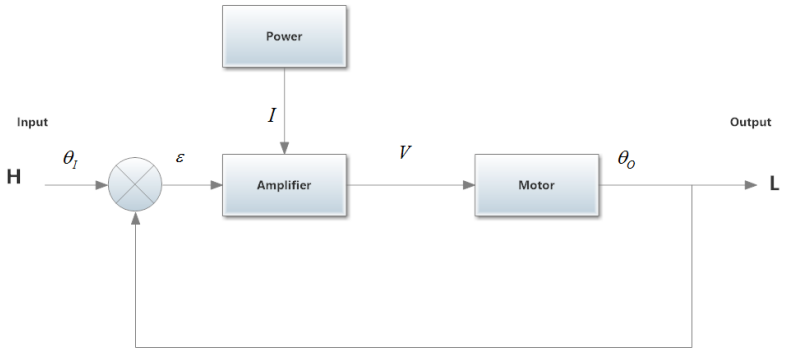

Figure 2.3: Closed loop system for a Servo motor. Picture idea from [Getting, 2015]

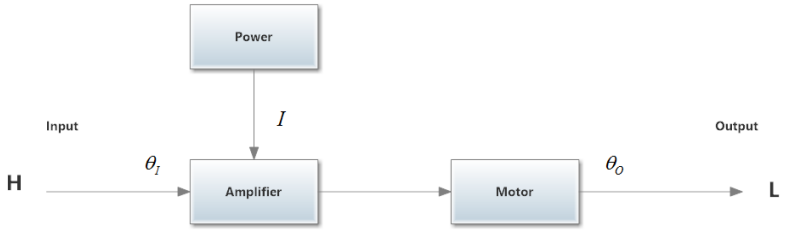

Figure 2.4: Open loop system for a DC motor. Picture idea from [Getting, 2015]

2.5 Time delay parameters

Each individual system generates a time delay from its output, which is important to account for in automation. The sensors work through reflection and the time the signal travels back after finding an object results in a delay

$$\tau_{sensor} = \tau_{ping}/2 \tag{2.6}$$

where equation 2.1 is applicable for both types, in general resulting in the sensor delay equation

$$\tau_{sensor} = \frac{r_T}{c}. \tag{2.7}$$

The velocity for sound in air was mentioned in chapter 2.2 and the velocity for light in air is $c_{light} = 299700000m/s$. The time delay from the ultrasonic sensor could affect in terms of milliseconds depending on the distance and has to be evaluated. The time delay from the infrared sensor is in factors of nanoseconds and does not cause measurable errors in trivial cases.

The servo motor's rotation contributes to a time delay depending on degree

$$\tau_{servo} = \alpha\theta \tag{2.8}$$

where α is an unknown parameter which all depends on the specific servo used. Unless the servo has a linear angular velocity, its power output results in a specific angular velocity depending on set rotational degree. The time delay from the servo motor can be acquired through experimental analysis.

The communication between the micro controller and the different subsystems is another source of delay. Each device connected to the micro controller has a specific I/O frequency. The micro controller contributes a time delay

$$\tau_{microcontroller} = \sum_{1}^{n} \tau_{device,n} \tag{2.9}$$

where n is the amount of active devices that contribute to a final time delay.

Chapter 3

Demonstrator

This chapter describes the electronics, hardware and software used in the project.

3.1 Problem Formulation

The problem is to create a mechanical claw within the scope and purpose of the project, some technical solutions have to be applied to various issues.

- The system has to be able to detect the diameter of the moving object with accuracy enough to grip it.
- The claw has to maintain a grip for objects with different diameters.
- Each sensor has to integrate with each other to provide an automatized execution, without stopping or stalling the system.
- Time delay in each part of the system has to be calculated and accounted for the final execution.
- The link between the claw and the arm has to be designed and positioned without interfering with the system's functions.

3.2 Electronics

The system in overall consists of a microcontroller, three sensors and a servo motor. A block diagram of the system can be seen in Fig. 3.1 and the wiring is visualized in Appendix A

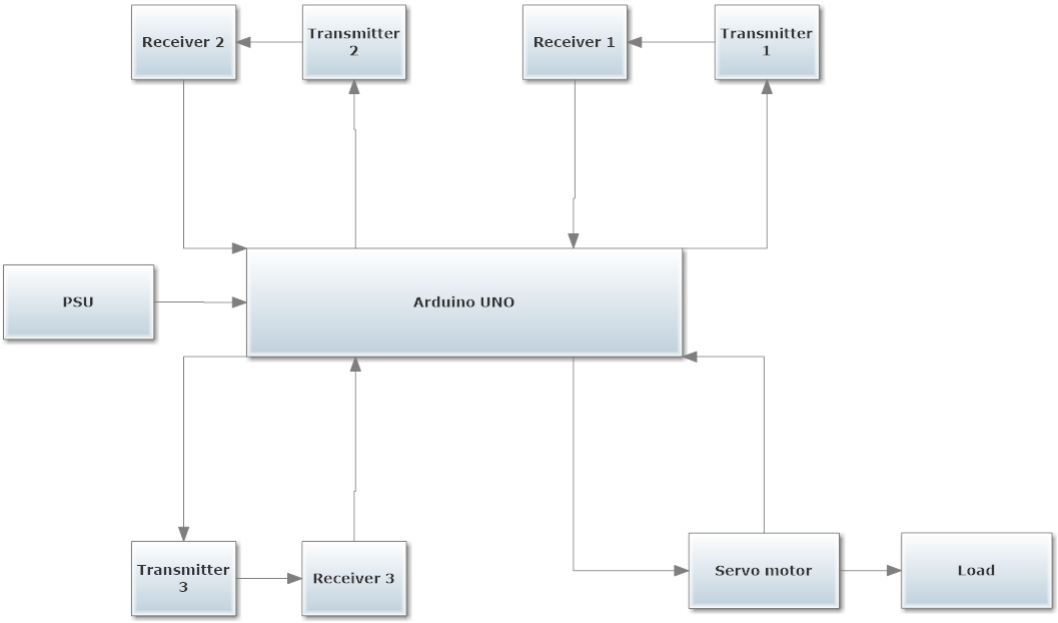

Figure 3.1: Block chart for the electronics.

3.2.1 Microcontroller - Arduino UNO

The Arduino UNO is an open source micro controller board based on the ATmega 328. The unit consists of 14 digital input/output pins, 6 with PWM abilities; 6 analog inputs, a 16 MHz ceramic resonator, a USB connection, an ICSP header, a power jack and a reset button. It is powered by 6 to 20 V and supplies 3.3 or 5 V as output power. The memory uses 32 KB with an additional 2 KB of SRAM and 1 KB of EEPROM. [Arduino, 2010]
The Arduino UNO acts as the CPU for the system and utilizes information from the input signals to control the automation. The different types and amount of pins on the micro controller satisfies the requirements for the rest of the electric components.

3.2.2 Ultrasonic Sensor - HC-SR04

Figure 3.2: Ultrasonic Sensor HCSR-04

The ultrasonic ranging module HC-SR04 is a digital sensor that provides a 2-400 cm measurement from ultrasonic waves. The device's modules include an ultrasonic transmitter, a receiver and a control circuit. The HC-SR04 has four pins. A VCC pin for 5 V power, a trigger pin for inputs to the module, an I/O echo pin connected to the receiver and a GND pin.
The sensor is triggered by a signal of at least $10\mu s$ that activates eight 40 kHz pulses from the transmitter. If the receiver registers a reflected signal back, it initiates a high output signal for a short duration.
The sensors act as detection devices and are placed a set distance away from the path of the objects at 90 °angle to the track,. To detect whether an object is on the track it measures the distance to the object with equation 2.1. The sensors are placed at a set distance between each other to enable time calculations for the moving object.
The sensor is a comfortable and viable option for distance measurements which could be utilized at a far range. A timing diagram can be seen in Fig. 3.3 . [elecfreaks, 2011]

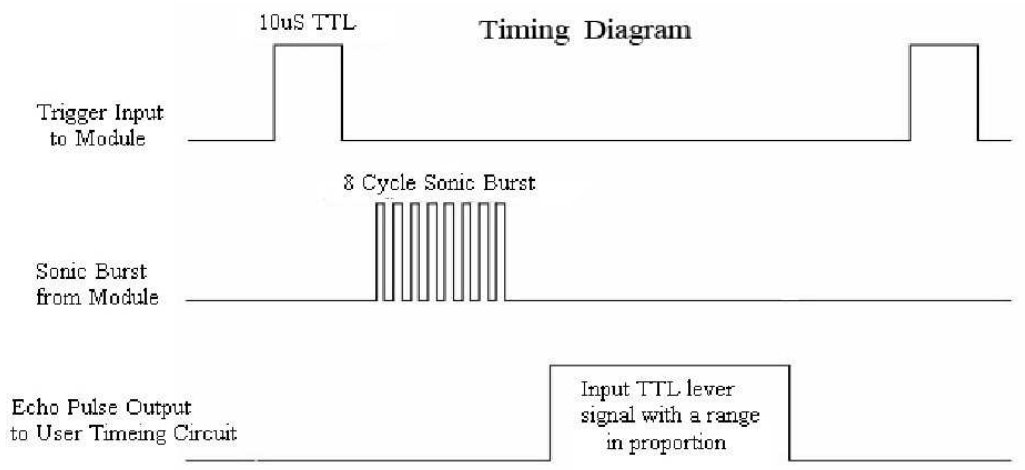

Figure 3.3: Timing diagram for the HC-SR04

3.2.3 Infrared Sensor - Sharp GP2Y0A21YK

Figure 3.4: Infrared sensor sharp GP2Y0A21YK0F

Sharp GP2Y0A21YK0F functions through infrared light for distance sensoring in range of 10-80 cm. It is of analog output functionality, is powered by 4.5-5.5V and has three pins; a Vcc pin for power, an I/O pin and a GND pin.
The sensor measures by varying the voltage output between 0-3.3V depending on distance. The further away from the sensor the target is, the lower the voltage becomes, as can be seen in Fig. 3.5. The measurements can become precise on a short range and give great results in correlation to the sensor's hardware. [Sharp, 2007] The IR sensor functions for the system is the same as the ultrasonic sensor mentioned in the section before.
Due to the analog bit output a conversion to desired unit has to be made. The conversion to centimeters can be made by

$$cm = \frac{5461}{analogoutput - 17} - 2. \tag{3.1}$$

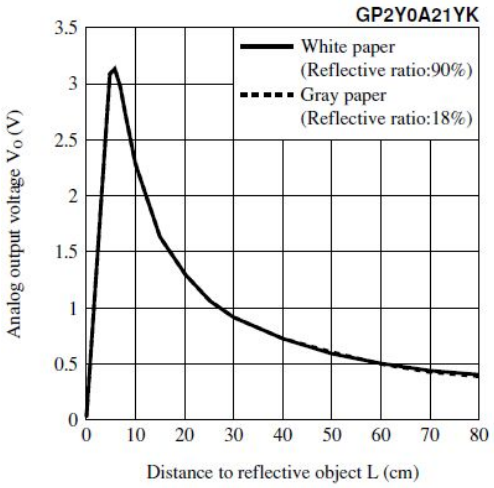

Figure 3.5: Voltage variation depending on distance for the sharp sensor.

3.2.4 Servo Motor - Parallax Standard Servo 900-00005

Parallax standard servo 900-00005 is a small servo with the ability to rotate 180°at a torque of 0.4 Nm. The servo has three pins; a Vcc pin for power between 4-6V, an I/O pin for 3.3-5V output signals and a GND pin. The servo motor is controlled by PWM signals and the position of the servo shaft, which grants the ability to thoroughly control the servo motor's rotation at any given time. The shaft is directly controlled by the duration of the pulse and a certain pulse length corresponds to a rotation angle. A pulse occurs every 20th ms and gives the ability to frequently control the angle of the servo shaft. [Parallax, 2012] An example of a time diagram of the servo can be seen in Fig. 3.6

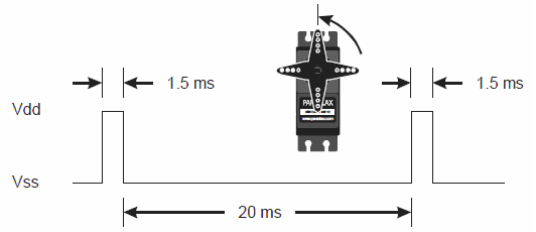

Figure 3.6: Sample time diagram for Parallax Standard Servo 900-00005.

3.3 Hardware

The hardware consists of the robot claw and the ramp used for the experiments. The material used consisted mainly of wood and EPS. A CAD figure of the complete claw can be seen in Fig. 3.7.

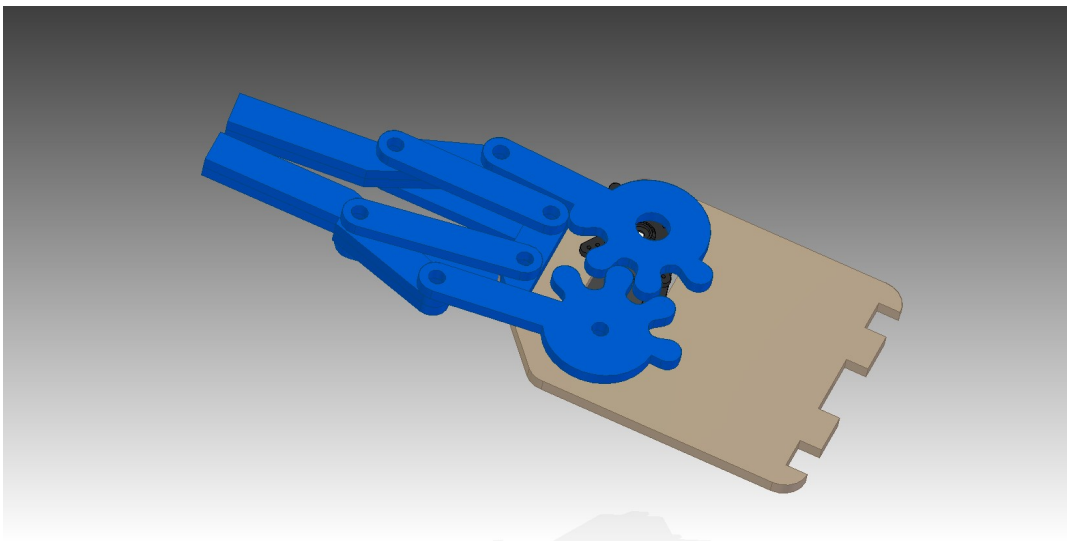

Figure 3.7: CAD model of the claw used in the project.

3.3.1 Robotic claw

The claw is based on and remodeled from a 3-D printing schematic acquired from the website www.thingsinverse.com and was created by the user "jjshortcut" [jjshortcut, 2015]. The size of each part was increased by 75 % with the height kept constant at 4 mm to scale it with the servo motor while maintaining functionality and low weight. The main component plate was extended to fit the micro controller.
The parts can be seen in Fig. 3.8 - 3.9 and consist of:

- A main component plate.
- Four straight bars.
- Four bent bars for gripping.
- Two bars with gears formed by their ends.
- Small bar for height adjustment.
- Small ring for height adjustment.

The robotic claw consists of a stationary part and a dynamic part. The stationary part is the main component plate. It is created out of plywood to maintain a low thickness to avoid interference with the dynamic parts. The sturdiness of the wood enables mounting a microcontroller, servo motor, dynamic parts and connecting it as an extension to construct of choice without breaking.

The dynamic part of the robotic claw is created with a 3D-printer out of EPS plastic to maintain light weight with low inertia. The bent bars are glued together to create a pair of bars to function as the direct gripping part of the claw. The edge of each bent bar is connected to the bars with gears. One of the gear bars are mounted to a servo motor by its cogwheel and the second is connected to the main plate on top of the small ring to adjust the height. The two gear bars are connected by their respective teeth, which enables a synchronized rotation for both sides.

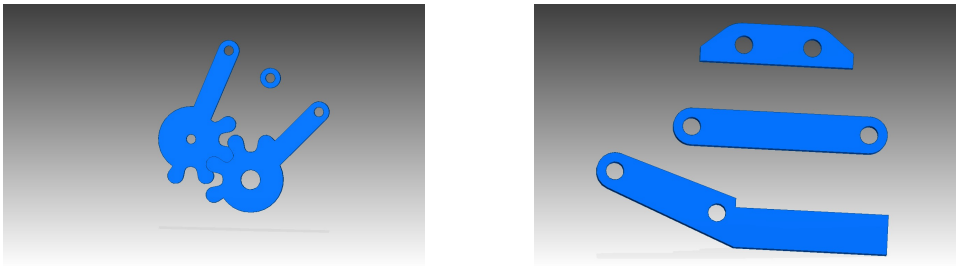

Figure 3.8: The different bars for the gripper. To the left are the gear bars with the height ring and to the right, from top to bottom; heigh adjustment bar, straight bar and bent grip bar.

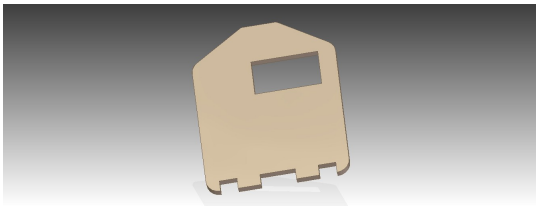

Figure 3.9: Picture of stationary main component plate. The rectangular hole is for servo placement.

The remaining four straight bars are used as a connection between the main plate and the gripping bars, one above and one below. The bars above rest on top of the small height adjustment bar to avoid asynchronism in the system. The straight bars keep the rest of the dynamic parts in place for the grip and adds stability. To enhance the friction of the grip, soft foam is applied to the lift bars.

3.3.2 Experimental set up

To be able to experiment on the robotic claw a set up that can vary the different parameters is necessary. It requires the function to generate a variety of velocities, different distances for sensor placement and maintain a one dimensional track for the moving object.
To fulfill the requirements a square formed ramp out of painted wood supported by pillars was constructed. The flat form keeps the track one dimensional and the painted wood lowers the frictional force to idealize the constraints set for the experiment. While supported by pillars, the slope of the ramp can be set at different angles which varies the velocity. Furthermore the remaining space can be used for sensor placement which gives a broad displacement range with minimized signal interference. A picture of the constructed ramp can be seen in Fig. 3.10 .
The holes were created to enable pillar placements for increased sturdiness depending on the sensor placement. The sensors were mounted on a piece of wood which enabled moving the sensors further away from the track while their displacements parallel to the track remained the same.

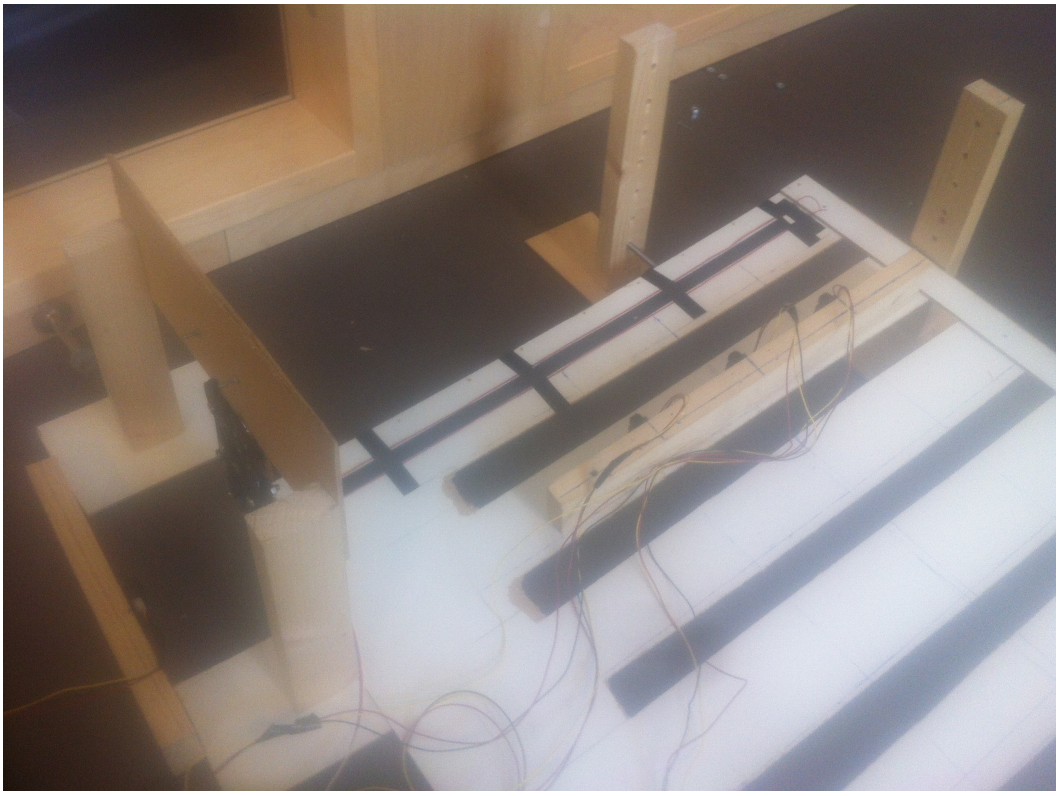

Figure 3.10: The ramp used for the experiments.

3.3.3 Robotic arm mount

The robotic claw is designed to work as an extension to a robotic arm currently in production by the mechatronic's master student Viktor Kozma from KTH. The structure of the strut, that becomes the edge of the arm, can be seen in Fig. 3.11 and is meant to move with two degrees of freedom where the motions are parallel with the ground. Therefor, the robotic claw has to be placed orthogonally on the edge of the strut. The strut's length is 300 mm and has height x width dimensions of 20x20 mm with a 5.5 mm diameter hole 14 mm from the edge of the strut. The mount between the robot claw and the arm has to be small yet sturdy.

To fulfill the requirements, four trapezoidal bars with 30 mm length made out of

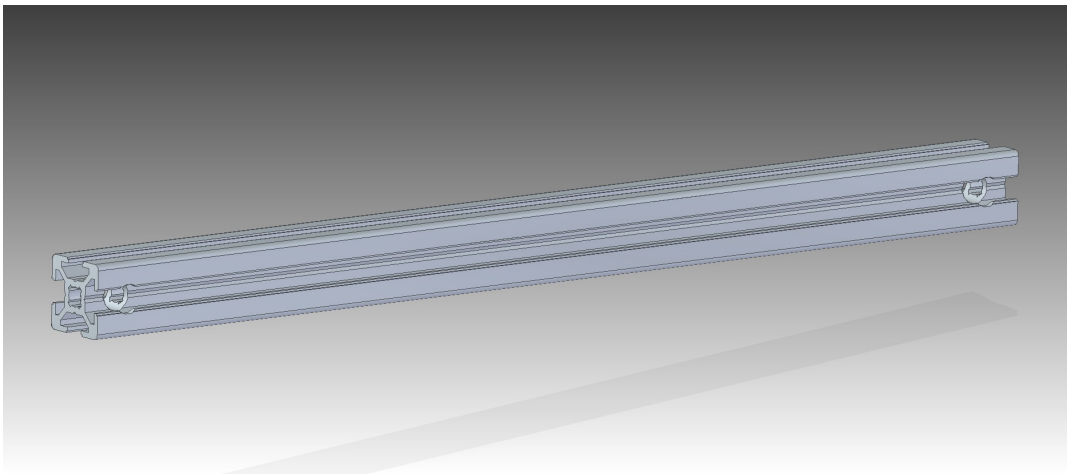

Figure 3.11: Strut profile for robotic arm.

wood are designed to fit in the trapezoidal holes of the strut. Additionally a 5.5 mm hole is made in the bars for a connecting part to avoid the claw to slip off the strut. An example design can be seen in Fig. 3.12

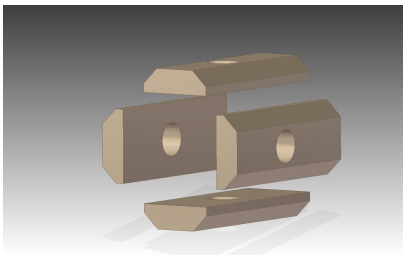

Figure 3.12: Connecting part for the claw and the arm.

3.4 Software

Overall the software predicts positioning through the sensors and translates the input into time through physic formulas in the Arduino UNO and processes an output to the servo motor, which in turn performs a motion at the correct time. The program functions with four main decision processes that activate subprocesses towards the final executional function of the program. A full flow chart of the software is pictured in Fig. 3.13 and descriptions of process explained below.

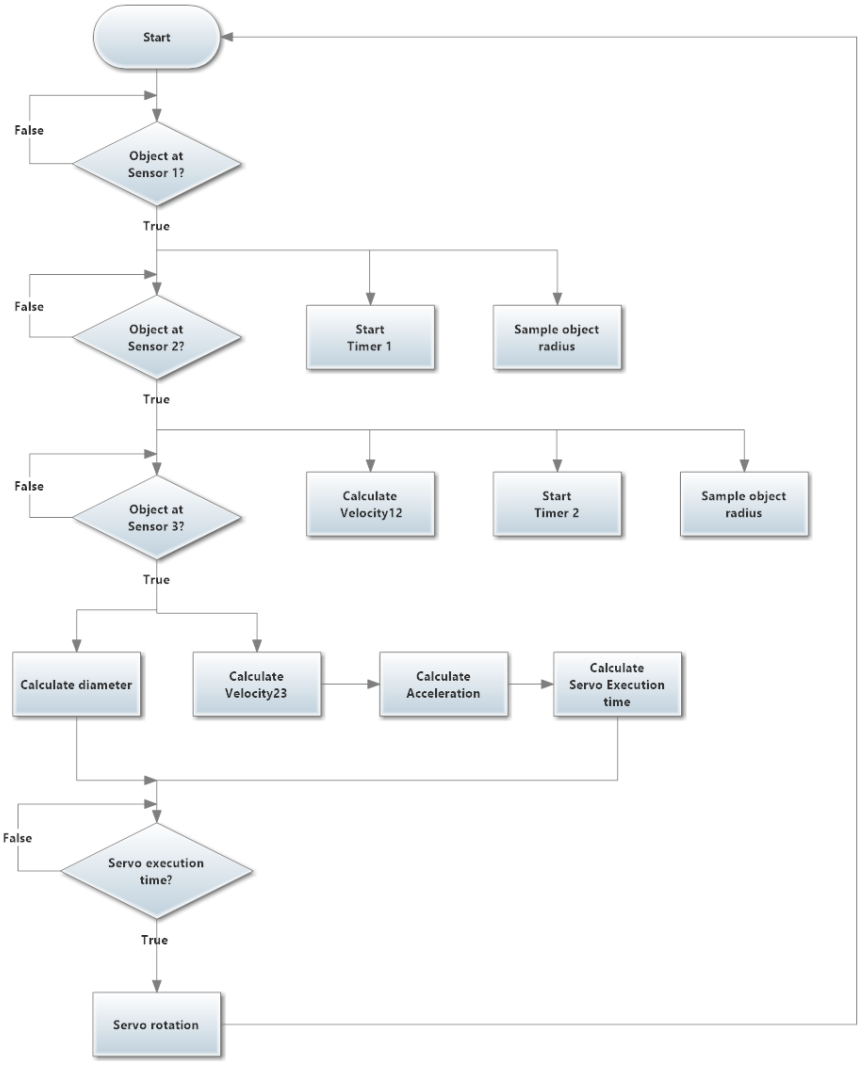

Figure 3.13: Flow chart for the software.

3.4.1 The first sensor

The first sensor determines whether an object is present within the object's path through measuring the distance to an object. When an object is found within the wanted distance range, the sensor sends a signal to the Arduino UNO to start a timer t_{12} and activate the second sensor's possibility to output its readings while its own abilities to send output disables. With the determined distance to the object and the orthogonal distance from the track it calculates one sample radius of the object.

3.4.2 The second sensor

The second sensor locates an object in the same way as the first. If the sensors finds an object the micro controller stops the timer t_{12}, calculates the mean velocity $\bar{v_{12}}$ between the two sensors from equation 2.3 where x_1 is the first sensor's position, x_2 is the second sensor's position and Δt is the timer t_{12}. The program starts a new timer t_{23} and activates the third sensor's output while disabling its own. With the same method as the first sensor it samples another radius for the object.

3.4.3 The third sensor

The third sensor's functions are the same regarding the readings. As an object is found it stops the recently started timer t_{23} and its regular output. The software calculates the mean velocity between the second and the third sensor through equation 2.3 with x_2 and the third sensor's position x_3. With calculated velocities and t_{23}, the mean acceleration of the object can be calculated with equation 2.2 The sensor samples a third and final radius. With the three different measurements the program calculates a mean diameter for the object which in turn determines a rotation angle for the servo motor.

3.4.4 The servo motor

The final procedure activates the servo motor to perform a mechanical grip with the claw at a precise moment with the calculated angle. The timing of the grip is calculated from the factors

- Time at position t_{34}, from the positive answer of equation 2.4.
- Time delay from third sensor's signal (see chapter 2.5).
- Time delay from servo rotation (see chapter 2.5).

which makes the servo rotation execute at the time

$$\tau_{execution} = t_{34} - \tau_{sensor,3} - \tau_{servo}. \tag{3.2}$$

3.5 Results

This chapter presents the results in two sections. The formulas derived from experiments with the claw and the experimental data received from tests.

3.5.1 Experimental formulas

Different servo angles are set between $\theta = 0, 5, 10, ..., 50$ and the diameter d of the grip position measured. The results are plotted and interpolated with Matlab, see Fig. 3.14. The function for angle based on diameter becomes

$$\theta = 7.4837d - 5.7653 \tag{3.3}$$

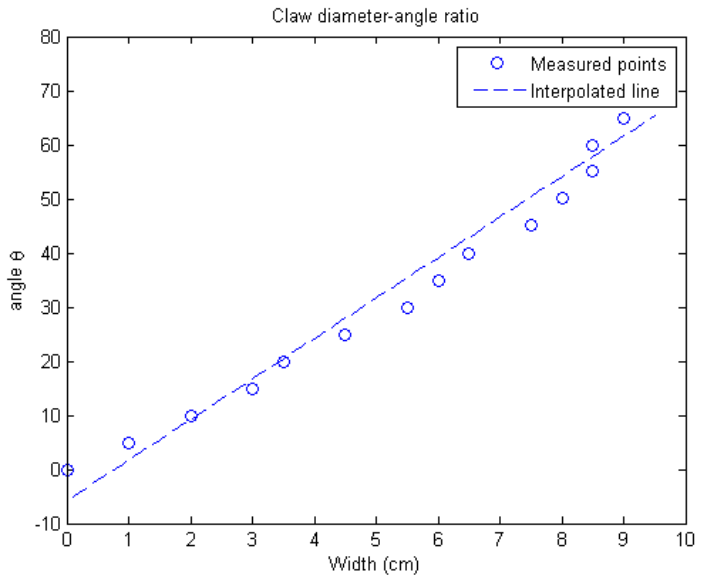

Figure 3.14: Interpolated graph with values of the angle as a function of the diameter.

The servo angles are set to rotate between 0 and a variable angle with a set time delay between the two executions. The time delay is lowered until the angle is unable to reach the diameter measured above. As an example the angles 0 °and 10 °are tested. The delay between the executions are set to 300 ms, 290 ms, 280 ms... and so on. When the time delay cannot be lowered without the claw getting a grip diameter lower than the measured diameter for 10 °the results are stored. With angles ranging from $\theta = 10, 20...50$ the results were plotted and interpolated with Matlab, see Fig. 3.15 . The function for the time delay based on angle becomes

$$\tau_{angledelay} = 0.1214\theta^2 - 2.3857\theta + 64 \tag{3.4}$$

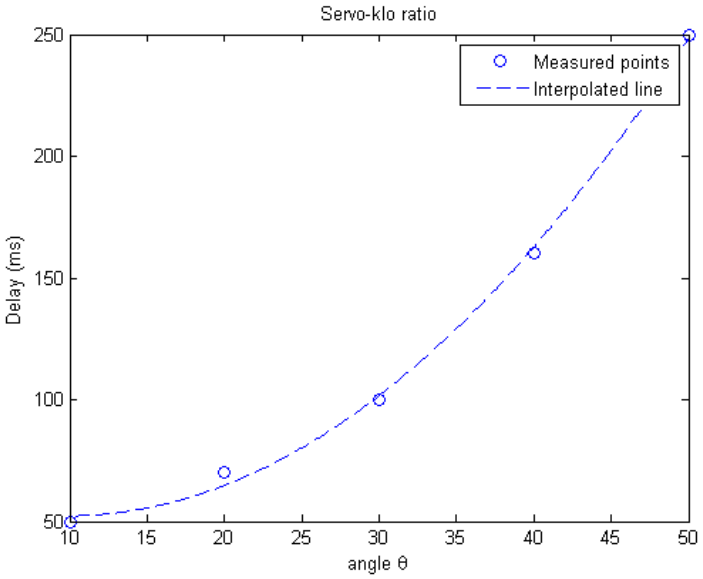

Figure 3.15: Interpolated graph with values of the time as a function of the angle

3.5.2 Experimental data

The measurements obtained from the experiments can be seen in Table 3.1 - 3.4 .

Table 3.1: Results for infrared sensor with varying the velocity and sensor distance to the track. $x_1 = 0cm$, $x_2 = 10cm$, $x_3 = 20cm$, $x_4 = 48cm$, $r = 1.25cm$.

Ramp angle $\theta(degrees)$	$v_{23}(m/s)$	Track $y(cm)$	Measured radius $r(cm)$	$\Delta t_{error}(s)$
4	0.558	11	1.1	-0.0284
4	0.552	11	0.83	-0.6884
4	0.592	11	0.988	0.1524
4	0.490	11	0.895	-0.0001
4	0.588	11	1.49	0.1187
4	0.621	19.5	1.09	-0.0007
4	0.621	19.5	1.07	0.1323
4	0.654	19.5	0.85	0.0643
4	0.591	19.5	0.925	0.0206
4	0.680	19.5	1.54	0.0698
4	0.574	26.5	1.54	0.0936
4	0.598	26.5	0.653	0.1499
4	0.568	26.5	0.785	0.0140
4	0.610	26.5	1.53	0.0758
4	0.575	26.5	4.155	0.1565
10.5	0.694	11	1.1	0.0324
10.5	0.806	11	0.495	0.0454
10.5	0.787	11	0.535	0.0873
10.5	0.870	11	0.525	0.1175
10.5	0.667	11	1.251	0.0306

Table 3.2: Results for infrared sensor with varying the velocity and sensor distance to the track. $x_1 = 0cm$, $x_2 = 10cm$, $x_3 = 20cm$, $x_4 = 48cm$, $r = 1.75cm$.

Ramp angle $\theta(degrees)$	$v_{23}(m/s)$	Track $y(cm)$	Measured radius $r(cm)$	$\Delta t_{error}(s)$
4	0.654	11	1.48	0.1114
4	0.610	11	1.03	0.0863
4	0.467	11	1.8	-0.471
4	0.606	11	2.02	0.0493
4	0.591	11	1.9	0.0745
4	0.592	19.5	1.63	0.1025
4	0.575	19.5	2.38	0.0626
4	0.610	19.5	1.63	0.0885
4	0.543	19.5	2.185	0.0558
4	0.526	19.5	0.61	0.0063
4	0.592	26.5	6.07	0.7089
4	0.483	26.5	4.35	0.1569
4	0.709	26.5	4.16	0.3377
4	0.610	26.5	5	0.5485
4	0.654	26.5	5.52	0.7179
10.5	0.763	11	1.9	0.0733
10.5	0.741	11	2.2	0.0708
10.5	0.704	11	1.23	0.0192
10.5	0.758	11	1.74	0.0964
10.5	0.877	11	1.52	0.1224

Table 3.3: Results for ultrasonic sensor with varying the velocity and sensor distance to the track. $x_1 = 0cm$, $x_2 = 10cm$, $x_3 = 20cm$, $x_4 = 48cm$, $r = 1.25cm$.

Ramp angle $\theta(degrees)$	$v_{23}(m/s)$	Track $y(cm)$	Measured radius $r(cm)$	$\Delta t_{error}(s)$
4	0.691	8.5	0.50	0.1514
4	0.615	8.5	0.49	0.1847
4	0.752	8.5	0.52	0.1977
4	0.652	8.5	0.25	0.1911
10.5	0.907	8.5	0.31	0.1209
10.5	0.686	8.5	1.09	0.0423
10.5	0.878	8.5	0.95	-0.0095
10.5	0.874	8.5	0.7	0.0805

Table 3.4: Results for ultrasonic sensor with varying the velocity and sensor distance to the track. $x_1 = 0cm$, $x_2 = 10cm$, $x_3 = 20cm$, $x_4 = 48cm$, $r = 1.75cm$.

Ramp angle $\theta(degrees)$	$v_{23}(m/s)$	Track $y(cm)$	Measured radius $r(cm)$	$\Delta t_{error}(s)$
4	0.593	8.5	0.25	0.1043
4	0.728	8.5	0.43	0.1826
4	0.644	8.5	0.34	0.1347
4	0.608	8.5	0.53	0.1304
10.5	0.900	8.5	0.33	0.1112
10.5	1.017	8.5	0.44	0.1923
10.5	0.951	8.5	0.25	0.1181
10.5	1.103	8.5	0.78	0.2150

Chapter 4

Discussion and conclusions

This chapter presents the discussions and conclusions drawn from the results presented in the previous chapter.

4.1 Discussion

The main factors that causes a time delay, discussed in chapter 2.5, relates to the software, different sensors and the servo motor. With the formula calculated in chapter 3.5.1 the errors generated from the servo motor should be within small margins, yet it's still a probable cause of time delays.

The simple motion formula applied in the software as a physical model is not ideal. Unless the path the object moves in is frictionless and the temperature remains constant in the specified area, some nonlinear accelerations may occur. The experiments were based on shorter lengths of motion in a smaller room. Any errors caused by either drag or friction should be proportional to the length of the track, which leads to a smaller error. Unless in an extreme case such as a jagged track or during a storm which realistically does not need to be considered.

The remaining source lies in the sensors. The largest issue is the signal reflections back to the sensors, which poses one unique problem for each sensor. The input to the infrared sensor's receiver is the intensity of the amount of the signal reflected back to the receiver which correlates to a certain voltage. Since the moving object is formed as a sphere, the reflections are spread and produce misleading information to the micro controller, which becomes obvious from the radius readings seen in Fig. 4.1 . The data becomes less accurate further away from the object, which indicates that a the intensity becomes less accurate the further away the sensor is placed. It would be the effect of additional proportions of light becoming scattered away from the receiver. The same indication is shown in Fig. 4.2 where the intensity of time delays is higher further away from the track.

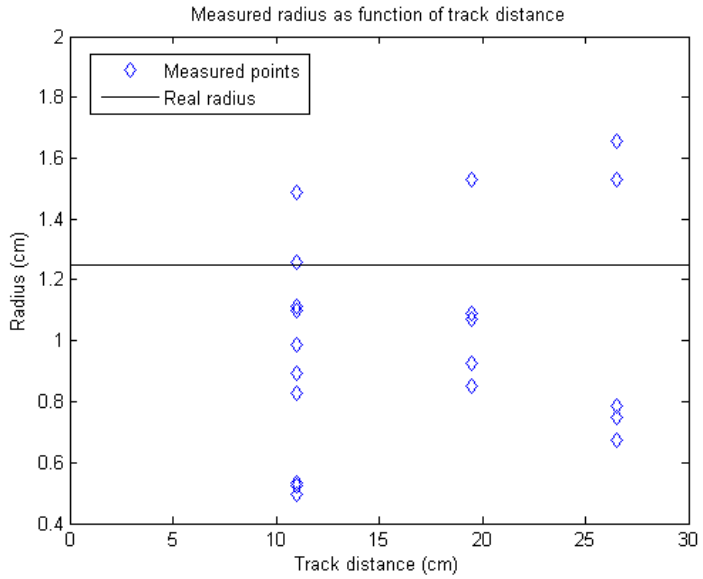

Figure 4.1: Radius-track distance data from the experiment with the IR-sensor.

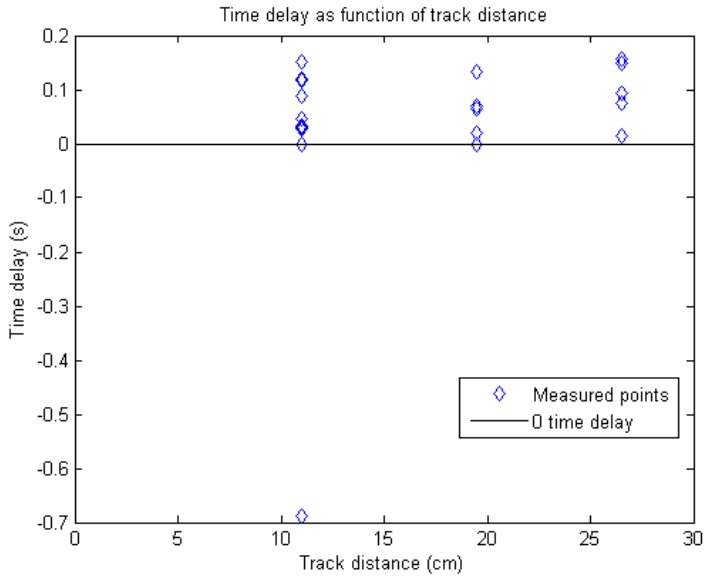

Figure 4.2: Time-track distance data from the experiment with the IR-sensor.

The ultrasonic sensor forms an error in result of its pulse which is distributed over a 30 °angle for the chosen sensor. Due to the electronics, it is unable to

pulse faster than a certain interval. It leads to an impossibility to determine where in this pulse it will encounter the moving object and results in an inaccuracy in both position and distance measurement, generating in spread data. Due to its properties, it was not fast enough to detect objects further than 10 cm away from the track position.
The difference in both sensors varied in time dependency due to the issues mentioned earlier, where the ultrasonic sensor contained few results within a low time delay, as can be seen in Fig. 4.3 . The inaccurate position determination that occurs from the ultrasonic sensor's broad wave acted too unpredictable compared to the smaller wave produced by the infrared sensor.

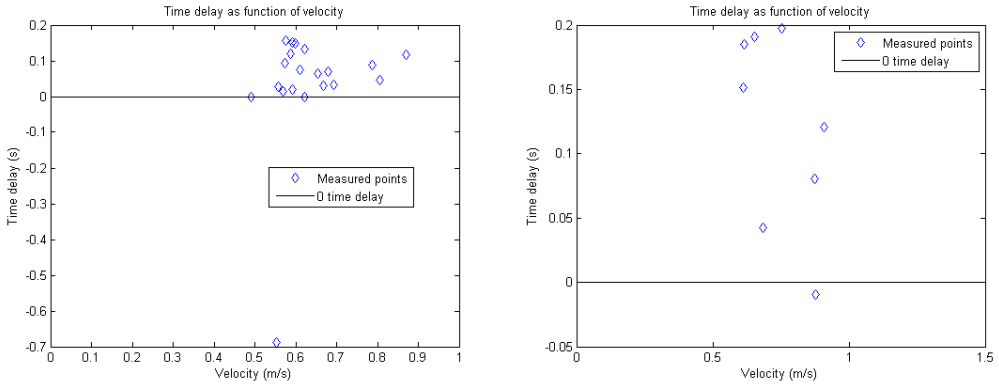

Figure 4.3: Infrared sensor in the left picture and ultrasonic right . Time delays as function of velocity for the two sensors using the 1.25 cm radius ball.

4.2 Conclusions

The radius measurements does not function as intended with the quality of neither sensor. The readings were not accurate enough, since the ultrasonic sensor could not determine the position of the object with precision and the IR-sensor received misleading intensity from the spherical surface. It would require a different type of sensor or shape of moving object to be able to detect the radius properly.

For motion automatized activation ultrasonic sensors are not an ideal choice due to its broad waves with slow feedback from the ultrasonic pulses. The object's position was not possible to determine with reliable accuracy and the sensors were constrained to either very slow motions or close range. The unpredictable properties of the sensor made it unable perform accurate execution unless the time frame would be large.

Infrared sensors possess easier configuration and more accurate results with its faster signals and function better for detection of moving objects. The accuracy becomes lower with further distance, but the point where it detects its object is reliable. By involving the time accuracy error of the specific sensor depending on distance from the track, it could perform a grip with high accuracy enough to function for catching moving objects.

Chapter 5

Recommendations and future work

The limitations and idealizations in this thesis leaves space to achieve more precise data and more accurate results. With this paper as reference, recommendations for future can be made in several areas. Although the claw is not fully up to its believed potential; the physical constructed claw, and to some extent its programming, could be applied as a subsystem in greater systems.

5.1 Recommendations

An improvement would be to increase the amount of sensors for the detection. Additional variables leads to options of more advanced physical models that can be applied to similar systems, such as Taylor expansion or Linear-quadratic regulator.

A more advanced sensor would reduce the signal delays and limit the inaccuracy in the readings, hence improve the current state of the system. An example would be a laser sensor, which would remove the intensity or position determination problems due to its precise detection properties.

5.2 Future work

To improve the readings required for the system to work with satisfactory accuracy, the IR-sensor's time error depending on the distance to the track has to be measured and discretized. It certainly requires

Bibliography

[Alpman, 2014] Alpman, M. (2014). Robotfabrik vÃ¤xer med enkel arm. Available from: http://www.nyteknik.se/nyheter/automation/verkstadsautomation/article3828553.ece [cited 2015-04-22].

[Arduino, 2010] Arduino (2010). Arduino uno. Available from: http://www.arduino.cc/en/Main/ArduinoBoardUno [cited 2015-05-12].

[Broman, 2015] Broman, D. (2015). Available from: https://www.kth.se/profile/dbro/.

[elecfreaks, 2011] elecfreaks (2011). Ultrasonic ranging module hc - sr04. Available from: http://www.micropik.com/PDF/HCSR04.pdf [cited 2015-04-22].

[Getting, 2015] Getting, I. (2015). Servo systems. Available from: https://www.jlab.org/ir/MITSeries/V25.PDF [cited 2015-04-22].

[jjshortcut, 2015] jjshortcut (2015). Available from: http://www.thingiverse.com/thing:2415.

[Karlsson, 2013] Karlsson, F. (2013). Robotarm skÃ¶tr det farliga jobbet. Available from: http://www.nyteknik.se/nyheter/automation/processautomation/article3759897.ece [cited 2015-04-22].

[Murdock, 2000] Murdock, D. (2000). One dimensional motion. Available from: http://iweb.tntech.edu/murdock/books/PreSci.pdf [cited 2015-04-22].

[Parallax, 2012] Parallax (2012). Parallax standard servo (900-00005). Available from: https://www.parallax.com/sites/default/files/downloads/900-00005-Standard-Servo-Product-Documentation-v2.2.pdf [cited 2015-04-22].

[RoboticsAcademy, 1999] RoboticsAcademy (1999). Ir sensor. Available from: http://www.education.rec.ri.cmu.edu/content/electronics/boe/ir_sensor/1.html#top [cited 2015-04-22].

[Sharp, 2007] Sharp (2007). Sharp gp2y0a21yk0f. Available from: https://www1.elfa.se/data1/wwwroot/assets/datasheets/28995-eng_tds.pdf [cited 2015-04-22].

[Wong, 2011] Wong, K. D. (2011). Ultrasonic range sensor. Available from: http://www.kerrywong.com/2011/01/22/a-sensitive-diy-ultrasonic-range-sensor/ [cited 2015-04-22].

Appendix A

Additional information

A.1 Electronical wiring schematic

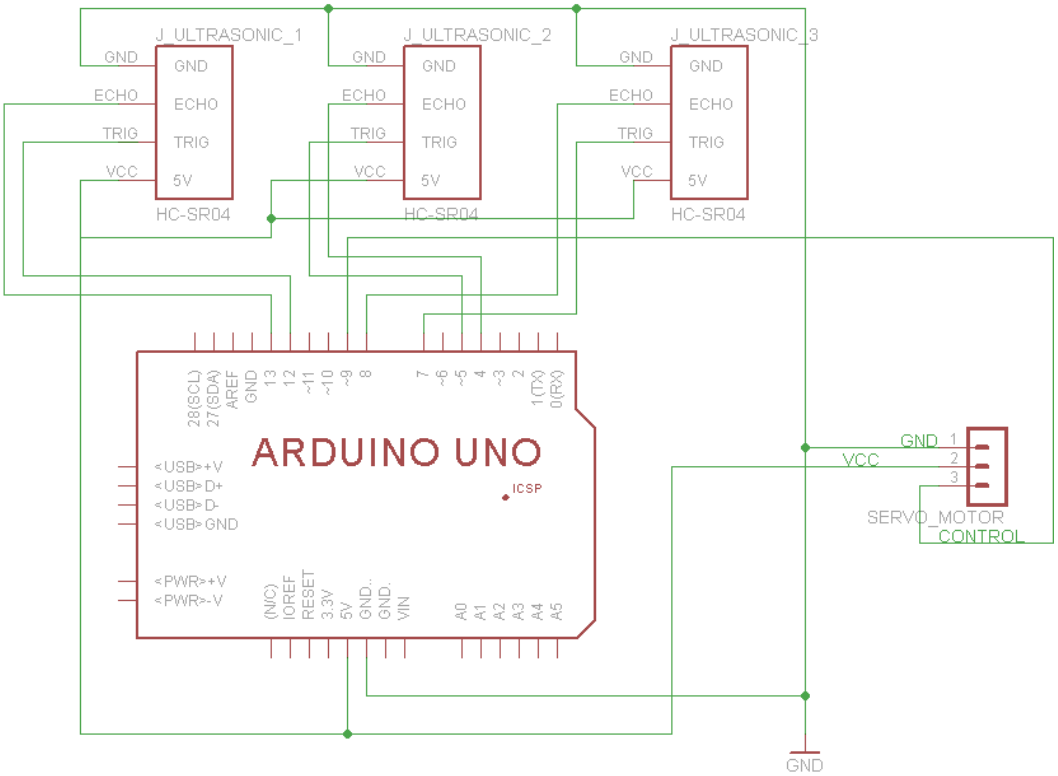

Figure A.1: Electrical wiring for the system created in EAGLE.

A.2 3D printing 2D schematic

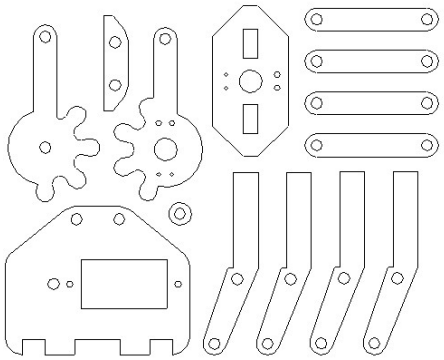

Figure A.2: 2-D picture with the different mechanical claw components.

TRITA MMK 2015:23 MDAB076